BIOLOGICAL CRYSTALLOGRAPHY
ISSN 1399-0047

3-Sulfinopropionyl-coenzyme A (3SP-CoA) desulfinase from *Advenella mimigardefordensis* DPN7^T: crystal structure and function of a desulfinase with an acyl-CoA dehydrogenase fold

Marc Schürmann,[a] Rob Meijers,[b] Thomas R. Schneider,[b] Alexander Steinbüchel[a] and Michele Cianci[b]*

[a]Institut für Molekulare Mikrobiologie und Biotechnologie, Westfälische Wilhelms-Universität Münster, 48149 Münster, Germany, and [b]European Molecular Biology Laboratory Hamburg Unit, EMBL, Notkestrasse 85, 22603 Hamburg, Germany. *Correspondence e-mail: michele.cianci@embl-hamburg.de

Received 9 February 2015
Accepted 1 April 2015

Edited by Z. S. Derewenda, University of Virginia, USA

Keywords: desulfinase; dehydrogenase fold; 3-sulfinopropionyl-coenzyme A; 3,3′-dithiodipropionic acid; arginine.

PDB references: 3-sulfinopropionyl-coenzyme A desulfinase, native, 5af7; complex with succinyl-CoA, 5ahs

Supporting information: this article has supporting information at journals.iucr.org/d

3-Sulfinopropionyl-coenzyme A (3SP-CoA) desulfinase (Acd_{DPN7}; EC 3.13.1.4) was identified during investigation of the 3,3′-dithiodipropionic acid (DTDP) catabolic pathway in the betaproteobacterium *Advenella mimigardefordensis* strain DPN7^T. DTDP is an organic disulfide and a precursor for the synthesis of polythioesters (PTEs) in bacteria, and is of interest for biotechnological PTE production. Acd_{DPN7} catalyzes sulfur abstraction from 3SP-CoA, a key step during the catabolism of DTDP. Here, the crystal structures of apo Acd_{DPN7} at 1.89 Å resolution and of its complex with the CoA moiety from the substrate analogue succinyl-CoA at 2.30 Å resolution are presented. The apo structure shows that Acd_{DPN7} belongs to the acyl-CoA dehydrogenase superfamily fold and that it is a tetramer, with each subunit containing one flavin adenine dinucleotide (FAD) molecule. The enzyme does not show any dehydrogenase activity. Dehydrogenase activity would require a catalytic base (Glu or Asp residue) at either position 246 or position 366, where a glutamine and a glycine are instead found, respectively, in this desulfinase. The positioning of CoA in the crystal complex enabled the modelling of a substrate complex containing 3SP-CoA. This indicates that Arg84 is a key residue in the desulfination reaction. An Arg84Lys mutant showed a complete loss of enzymatic activity, suggesting that the guanidinium group of the arginine is essential for desulfination. Acd_{DPN7} is the first desulfinase with an acyl-CoA dehydrogenase fold to be reported, which underlines the versatility of this enzyme scaffold.

1. Introduction

Degradation of 3-sulfinopropionyl-coenzyme A (3SP-CoA) into sulfite and propionyl-CoA is the last step in the 3,3′-dithiodipropionic acid (DTDP) bacterial catabolic pathway (Fig. 1). DTDP is an organic disulfide and a precursor for the synthesis of polythioesters (PTEs; Lütke-Eversloh & Steinbüchel, 2003). Elucidation of the degradation pathway of DTDP in *Advenella mimigardefordensis* strain DPN7^T and identification of the genes involved has been performed with the aim of providing a strategy to engineer strains suitable for biotechnological PTE production (Schürmann *et al.*, 2011, 2013; Wübbeler *et al.*, 2008, 2010; Bruland *et al.*, 2009). Recently, the isolation of a desulfinase (EC 3.13.1.4) catalyzing sulfur abstraction from 3SP-CoA during DTDP catabolism in the betaproteobacterium *Advenella mimigardefordensis* strain DPN7^T was reported (Schürmann *et al.*, 2013). The purified

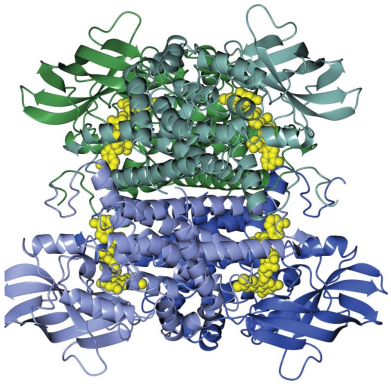

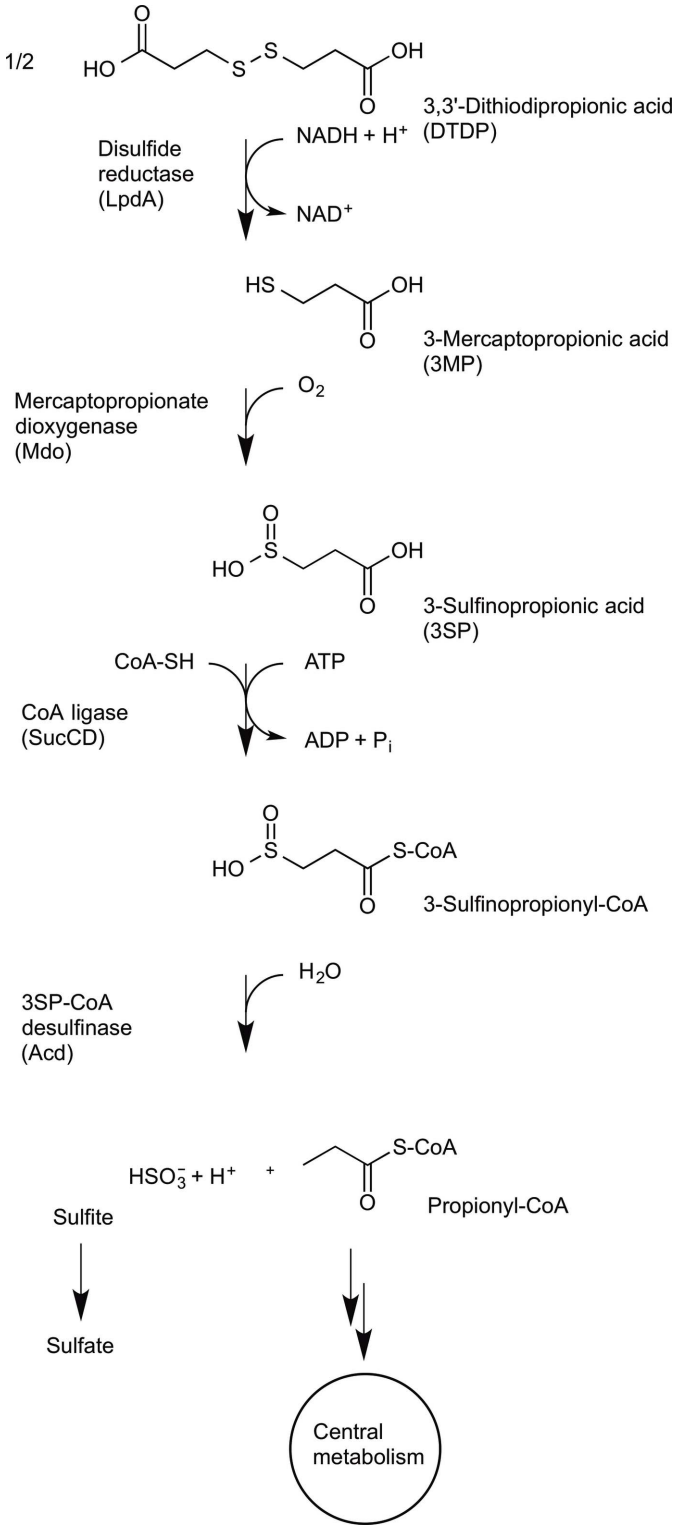

Figure 1
Degradation of DTDP. The disulfide 3,3′-dithiodipropionic acid (DTDP) is cleaved into two molecules of 3-mercaptopropionic acid (3MP) by an NADH-dependent disulfide reductase (Wübbeler *et al.*, 2010). After oxygenation of 3MP to 3-sulfinopropionic acid (3SP) by a dioxygenase (Mdo; Bruland *et al.*, 2009), a succinate-CoA ligase (SucCD; Schürmann *et al.*, 2011) catalyzes the activation to 3SP-CoA. Subsequently, 3SP-CoA desulfinase (Acd) catalyzes the hydrolytic cleavage, yielding propionyl-CoA and sulfite. Propionyl-CoA finally enters the central metabolism *via* the methyl citric acid cycle, while sulfite is most probably oxidized to sulfate by sulfite oxidases.

protein showed a native molecular mass of about 150–200 kDa, indicating a homotetrameric structure, and it contained one noncovalently bound flavin adenine dinucleotide (FAD) cofactor per subunit, which is in accordance with other members of the acyl-CoA dehydrogenase superfamily (Schürmann *et al.*, 2013). In a previous study, *in vitro* assays confirmed that the purified enzyme converted 3SP-CoA into propionyl-CoA and sulfite, but it was unable to perform a dehydrogenation (Schürmann *et al.*, 2013), which is the usual reaction catalyzed by members of the acyl-CoA dehydrogenase (Acd) superfamily (EC 1.3.8.*x*).

More recently, Acd_{TBEA6} from *Variovorax paradoxus*, Acd_{LB400} from *Burkholderia xenovorans* and Acd_{N-1} from *Cupriavidus necator* were identified as 3SP-CoA desulfinases within the acyl-CoA dehydrogenase family, with about 60% sequence identity to Acd_{DPN7}. None of these three Acds dehydrogenated any of the tested acyl-CoA thioesters, *i.e.* butyryl-CoA, isobutyryl-CoA, valeryl-CoA, isovaleryl-CoA, glutaryl-CoA, succinyl-CoA and 3SP-CoA (Schürmann *et al.*, 2014).

In addition to these new desulfinases, three other bacterial enzymes have been reported to date which catalyze desulfination reactions on various substrates, yielding sulfite as one of the end products. One is the pyridoxal phosphate (PLP)-dependent cysteine sulfinate desulfinase (CSD; EC 4.4.1.16) from *Escherichia coli*, which has selenocysteine lyase and cysteine desulfurase side activities (Mihara *et al.*, 1997). The second is a PLP-dependent aspartate β-decarboxylase (EC 4.1.1.12), which can accept cysteine sulfinate and catalyzes desulfination as a side reaction (Fernandez *et al.*, 2012). The third enzyme, DszB (EC 3.13.1.3), catalyzes the hydrolysis of a sulfinate group from 2′-hydroxybiphenyl-2-sulfinate as well as from 2-phenylbenzene sulfinate (Nakayama *et al.*, 2002; Lee *et al.*, 2006). None of the reported desulfinases show structural similarities to the Acds (EC 1.3.8.*x*).

Acds belong to a superfamily of flavoenzymes that mainly catalyze the α,β-dehydrogenation of acyl-CoA thioesters using electron-transferring flavoproteins (ETFs) as their physiological electron acceptors (Kim & Miura, 2004). Acds are involved mainly in fatty-acid oxidation or in branched-chain amino-acid metabolism, but also in less common bacterial metabolic pathways. Examples are the benzylsuccinyl-CoA dehydrogenase from *Thauera aromatica* involved in the anaerobic toluene catabolic pathway (Leutwein & Heider, 2002) and the 2-methylsuccinyl-CoA dehydrogenase (Mcd) involved in the ethylmalonyl-CoA pathway (Erb *et al.*, 2009).

Here, we report two crystal structures of the 3SP-CoA desulfinase Acd_{DPN7}. The crystal structure of the apoenzyme at 1.89 Å resolution reveals a fold typical of the acyl-CoA dehydrogenase superfamily. More specifically, Acd_{DPN7} is a tetramer and each monomer has one FAD noncovalently bound to the polypeptide. Co-crystallization with succinyl-CoA resulted in a holo complex containing CoA. This structure at 2.30 Å resolution shows how CoA is bound and provides clues with respect to substrate binding. The crystal structure reveals the configuration of the residues around the active site and indicates a prominent role for Arg84 in

desulfination. Mutagenesis shows that Arg84 is essential and structural comparisons provide insights into how a desulfinase might have appeared within the dehydrogenase superfamily.

2. Materials and methods

2.1. Chemicals

3SP of at least 95% purity, according to gas chromatography (GC), was synthesized using a method described previously by Jollés-Bergeret (1974) but modified by repeating the step for the alkaline cleavage of the bis-(2-carboxyethyl)sulfone intermediate (Wübbeler *et al.*, 2008, 2010). The synthesis and purity of 3SP was analyzed by GC and GC/MS as described elsewhere (Schürmann *et al.*, 2011; Wübbeler *et al.*, 2008). *In situ* formation of 3SP-CoA, which was also not commercially available, for enzyme assays was performed according to a method described elsewhere (Schürmann *et al.*, 2014). Other CoA thioesters, namely propionyl-CoA, butyryl-CoA, isobutyryl-CoA, valeryl-CoA, isovaleryl-CoA, succinyl-CoA and glutaryl-CoA, were synthesized by a modified technique based on the anhydride method of Simon & Shemin (1953). This modified method has been described previously (Schürmann *et al.*, 2013, 2014).

2.2. Isolation, manipulation and transfer of DNA

High-purity plasmid DNA of *E. coli* was obtained by employing the peqGOLD Plasmid Miniprep Kit I (Peqlab Biotechnologie GmbH, Erlangen, Germany), whereas plasmid DNA of lower quality was isolated based on the method of Birnboim & Doly (1979). Purification of DNA fragments or plasmid DNA by gel extraction was carried out using the PureExtreme GeneJet gel-extraction kit from Fermentas GmbH (St Leon-Rot, Germany) according to the manufacturer's manual. Restriction endonucleases for DNA digestion were also purchased from Fermentas GmbH and were utilized as instructed. Phusion High-Fidelity DNA Polymerase obtained from the same company served for PCR-based amplifications, which were performed with a peqSTAR 2X Gradient Thermocycler (Peqlab Biotechnologie GmbH, Erlangen, Germany). The required primers (Supplementary Table S1) were synthesized by MWG-Biotech AG (Ebersberg, Germany). Ligations were carried out using T4 DNA ligase from Fermentas GmbH (Schwerte, Germany). The preparation and transformation of competent *E. coli* cells was performed according to the $CaCl_2$ method as described by Sambrook *et al.* (1989). DNA sequencing was carried out by Seqlab (Göttingen, Germany) and the obtained sequences were analyzed using the *BLAST* tool of the NCBI server (National Center for Biotechnology Information; http://www.ncbi.nlm.nih.gov/BLAST/; Altschul *et al.*, 1997).

The plasmid pET-23a::*acd*$_{DPN7}$ was used as a template for the construction of mutant plasmids for the expression of Acd_{DPN7} variants (Schürmann *et al.*, 2013). PCR amplification was performed using Phusion DNA polymerase (Fisher Scientific GmbH, Schwerte, Germany). Two phosphorylated primers (see Supplementary Table S1), one of which carried the mutated DNA sequence, were used to amplify the whole plasmid. The PCR was performed in Phusion High Fidelity buffer supplemented with 1%(*v*/*v*) DMSO. After initial denaturation at 98°C for 4 min, samples were subjected to 30 cycles of denaturation at 98°C for 20 s, annealing at 61–64°C for 30 s and elongation at 72°C for 2.5 min in a peqSTAR 2X Gradient Thermocycler. The PCR product was purified from an agarose gel, ligated with T4 DNA ligase from Fermentas GmbH (Schwerte, Germany) and subsequently transformed into $CaCl_2$-competent *E. coli* Top10 cells. Positive clones carrying the desired mutations were identified by DNA sequencing of plasmid DNA. Plasmids were then transformed into $CaCl_2$-competent cells of the expression strain *E. coli* BL21 (DE3) pLysS.

2.3. Expression and purification of Acd_{DPN7} and enzyme variants

Expression of Acd_{DPN7} and enzyme variants took place in *E. coli* BL21 (DE3) pLysS cells carrying the appropriate plasmid as described previously (Schürmann *et al.*, 2013). Cells were subsequently harvested by centrifugation (15 min at 4°C and 3400*g*) and washed twice with sterile saline solution. The supernatant was discarded and the pellet was stored at −20°C. For His_6-tag purification, the cells were resuspended in binding buffer (100 m*M* Tris–HCl, 500 m*M* sodium chloride, 20 m*M* imidazole pH 7.4). Lysis was performed by a threefold passage through a cooled French press at 100 MPa. The soluble protein fraction was obtained after 1 h of centrifugation at 10 000*g* at 4°C. His SpinTrap affinity columns (catalogue No. 28-4013-53; GE Healthcare, Uppsala, Sweden) served for the purification of the small amounts of enzyme required for initial tests following the manufacturer's instructions. For this, Ni–nitrilotriacetic acid (NTA) columns were equilibrated with the abovementioned binding buffer. The washing step was carried out using a buffer of the same composition and pH but containing 40 m*M* imidazole, whereas the elution buffer required a 500 m*M* concentration of imidazole. For large-scale purification, two HisTrap HP columns of 1 ml in volume were serially connected (catalogue No. 17-5247-01; GE Healthcare, Uppsala, Sweden) and were equilibrated with five volumes of the abovementioned binding buffer. Subsequently, two washing steps were performed using buffer of the same composition but with imidazole concentrations of 100 and 150 m*M*, resulting in higher protein purity. The protein was eluted with 500 m*M* imidazole. The purified protein was stored at a concentration of 2 mg ml^{-1} and at −20°C in elution buffer complemented with glycerol to a final concentration of 50%(*v*/*v*). Protein concentrations were determined according to Bradford (1976).

To further enhance the purity prior to crystallization, Acd_{DPN7} was subjected to a size-exclusion chromatography step. A Superdex 200 HP 16/600 column was equilibrated with 20 m*M* sodium phosphate buffer containing 150 m*M* sodium chloride at an adjusted pH of 7.4. Calibration was carried out using a high-molecular-mass gel-filtration calibration kit (catalogue No. 28-4038-42; GE Healthcare, Uppsala, Sweden)

including ovalbumin (44 kDa), conalbumin (75 kDa), aldolase (158 kDa) and ferritin (440 kDa) by following the manufacturer's manual. The column was loaded with a total volume of 1 ml containing the purified enzyme. Chromatography was performed at a constant flow rate of 1 ml min^{-1}. Determination of the elution volume was achieved by following the absorbance at 280 nm. Samples containing Acd_{DPN7} were collected, pooled and buffer-exchanged into 10 m*M* HEPES buffer pH 7.4.

2.4. Enzyme assays

For examination of the desulfinase activity, the substrate 3SP-CoA was synthesized according to a previously described procedure (Schürmann *et al.*, 2014). A continuous spectrophotometric assay utilized the reaction of 5,5′-dithiobis(2-nitrobenzoic acid) (DTNB) with sulfite (Sadegh & Schreck, 2003), resulting in an increase in absorption at 412 nm ($\varepsilon_{412\ nm}$ = 14 150 M^{-1} cm^{-1}; Riddles *et al.*, 1983). Kinetic activity was determined in triplicate utilizing an assay containing 0.2 m*M* DTNB and 3SP-CoA at various concentrations (0.2, 0.15, 0.1, 0.075, 0.05, 0.025, 0.0125, 0.0075, 0.005 and 0.0025 m*M*) at a temperature of 30°C in 50 m*M* Tris–HCl pH 7.4. The reaction was started by adding 10 µl of the purified enzyme, resulting in a final protein concentration of 2 µg ml^{-1} (44.6 n*M*), unless stated otherwise. One unit of activity corresponds to the amount of enzyme that catalyzes the conversion of 1 µmol of substrate in 1 min.

To investigate the ability of an Acd_{DPN7_Q246E} mutant to catalyze the dehydrogenation of various acyl-CoA thioesters (propionyl-CoA, butyryl-CoA, isobutyryl-CoA, valeryl-CoA, isovaleryl-CoA, 3SP-CoA, succinyl-CoA and glutaryl-CoA), a ferrocenium hexafluorophosphate-based assay was utilized as described previously (Schürmann *et al.*, 2014). Briefly, the assay contained 0.2 m*M* ferrocenium hexafluorophosphate and 0.1 m*M* of the respective CoA thioester in 50 m*M* Tris–HCl pH 7.4 with a final volume of 1 ml and with a final enzyme concentration of 2 µg ml^{-1} (44.6 n*M*). The absorption was observed at 300 nm (ε_{300} = 4.3 M^{-1} cm^{-1}; Lehman *et al.*, 1990).

2.5. Oxygen-independency of Acd_{DPN7}

The potential oxygen-dependency of Acd_{DPN7} was assessed as follows. The assay solution contained final concentrations of 0.2 m*M* DTNB and 0.1 m*M* 3SP-CoA in a total volume of 1 ml 50 m*M* Tris–HCl pH 7.4 within a cuvette equipped with a rubber seal (117.104-QS, path length 10 mm; Hellma Analytics, Müllheim, Germany). A 950 µl assay solution was made anaerobic or oxygen-saturated by flushing with nitrogen or oxygen, respectively, for 5 min. Simultaneously, a solution containing Acd_{DPN7} in 50 m*M* Tris–HCl pH 7.4 was made anaerobic by flushing with nitrogen. Next, the solution was cooled on ice within a glass vial equipped with a rubber seal (catalogue Nos. 548-0028 and 548-0032, VWR International GmbH, Darmstadt, Germany). The headspace was flushed with nitrogen for 10 min *via* an inlet needle connected to a gas cylinder. A second needle (outlet needle) served to avoid overpressurization. Finally, the activity of Acd_{DPN7} in the absence and presence of oxygen was followed using the continuous spectroscopic assay described above. After preincubation at 30°C for 1 min, the assay was started by addition of 50 µl of the oxygen-free enzyme solution. The increase in absorption at 412 nm was followed for an additional 9 min. The absence or presence of oxygen was measured with an oxygen microrespiration sensor (OX-MR, Unisense, Aarhus, Denmark) connected to a picoammeter (PA2000, Unisense, Aarhus, Denmark) according to the manufacturer's instructions. The sensor was calibrated using H_2O saturated with compressed air (284 µ*M* O_2 at 20°C) and a solution of 0.1 *M* sodium ascorbate/0.1 *M* NaOH in water (0 µ*M* O_2 at 20°C).

2.6. Activity of Acd_{DPN7} with $FADH_2$

We tested whether Acd_{DPN7} could still catalyze the desulfination of 3SP-CoA when the FAD cofactor was reduced to $FADH_2$. To avoid the reoxidation of $FADH_2$ to FAD by oxygen, all procedures and measurements were performed in an anaerobic chamber (type A, manual air lock; Coy Inc., Grass Lake, Michigan, USA) containing an atmosphere of Formier gas [N_2:H_2, 95:5%(*v*:*v*)]. The chamber was equipped with an oxygen and hydrogen analyzer (model 10; Coy Inc., Grass Lake, Michigan, USA) to ensure operation at an oxygen concentration of 0 p.p.m.. Oxygen was removed from all solutions by flushing them with nitrogen before they were transferred into the anaerobic chamber. The only exceptions were the protein solutions, from which oxygen was removed as described in the previous section. Acd_{DPN7} was titrated with 10 m*M* sodium dithionite in 50 m*M* Tris–HCl buffer pH 7.4 to reduce the cofactor to $FADH_2$. The assay solution contained a final concentration of 0.2 m*M* DTNB and 0.2 m*M* 3SP-CoA in a total volume of 1 ml 50 m*M* Tris–HCl pH 7.4. The temperature was kept at 7°C. The assay was started by the addition of 10 µl enzyme solution. The increase in absorption was followed at 412 nm for 10 min.

2.7. Crystallization of native Acd_{DPN7} and its complex with succinyl-CoA and crystal mounting

Purified Acd_{DPN7} was initially crystallized by vapour diffusion in a sitting-drop configuration at a protein concentration of 13 mg ml^{-1} using The Classics II Suite (Qiagen) condition D10 [0.1 *M* Bis-tris pH 6.5, 20%(*w*/*v*) polyethylene glycol monomethyl ether 5000] by mixing 400 nl protein solution with 400 nl mother liquor. The crystals were further optimized, and the crystals used for X-ray diffraction studies were grown in 24-well Linbro plates (Hampton Research) by vapour diffusion in a hanging-drop configuration from 0.1 *M* Bis-tris pH 6.5, 5–20% PEG 3350 at a protein concentration of 10 mg ml^{-1} by mixing 2 µl protein solution with 2 µl mother liquor. The native Acd_{DPN7} crystals were cryoprotected by dipping the crystals into a solution containing 10% glycerol, 0.1 *M* Bis-tris buffer pH 6.5, 20% PEG 3350. To obtain the complex of Acd_{DPN7} with the substrate analogue, the Acd_{DPN7} protein was first crystallized in the presence of 4 m*M* succinyl-CoA (Sigma–Aldrich catalogue No. S1129) and then soaked in a solution that contained 10 m*M* succinyl-CoA as well as a

Table 1
Data-collection, processing and refinement statistics for the Acd_{DPN7} apoenzyme and its complex with CoA.

Values in parentheses are for the highest resolution bin.

	Native	Complex
Data collection		
Wavelength (Å)	0.968	0.968
Detector	Rayonix 225HE CCD	Pilatus 6M
Crystal-to-detector distance (mm)	183.6	441.7
Oscillation angle (°)	0.5	0.2
No. of images	360	1000
Space group	$P2_12_12$	$P2_12_12$
Unit-cell parameters (Å)	a = 75.6, b = 100.6, c = 118.5	a = 100.0, b = 233.4, c = 121.2
Resolution range (Å)	100.65–1.89 (1.93–1.89)	121.29–2.30 (2.34–2.30)
Total No. of reflections	225458 (14471)	617576 (30954)
Unique reflections	69785 (4549)	126487 (6219)
Multiplicity	3.2 (3.2)	4.9 (5.0)
Completeness (%)	96.0 (97.8)	99.9 (99.9)
R_{merge}† (%)	9.9 (72.6)	8.5 (94.7)
$R_{p.i.m.}$‡ (%)	5.1 (38.1)	5.1 (56.4)
Mean I half-set correlation $CC_{1/2}$	0.997 (0.684)	0.998 (0.816)
Mean $I/\sigma(I)$	12.1 (2.0)	13.5 (2.0)
Refinement statistics		
No. of monomers in the asymmetric unit	2	6
R factor§ (%)	16.2	19.9
R_{free}§ (%)	20.1	24.4
Cruickshank's DPI for coordinate error¶ based on R factor (Å)	0.1	0.3
Wilson plot B factor (Å^2)	19.0	40.8
Average all-atom B factor†† (Å^2)	22.3	54.5
R.m.s.d., bonds§ (Å)	0.01	0.002
R.m.s.d., angles§ (°)	1.12	0.6
Total No. of atoms‡	6920	19886
Total No. of water molecules	831	1462
Solvent content (%)	54.0	55.8
Matthews coefficient (Å^3 Da^{-1})	2.6	2.7
Ramachandran plot‡‡ (%)		
Most favoured region	94.2	94.0
Additionally allowed region	5.8	5.9
Generously allowed region	0.0	0.1
Disallowed region	0.0	0.0

† $R_{merge} = \sum_{hkl}\sum_i |I_i(hkl) - \langle I(hkl)\rangle| / \sum_{hkl}\sum_i I_i(hkl)$, where $I_i(hkl)$ is the intensity of a reflection and $\langle I(hkl)\rangle$ is the mean intensity of all i symmetry-related reflections. ‡ $R_{p.i.m.} = \sum_{hkl}\{1/[N(hkl)-1]\}^{1/2}\sum_i |I_i(hkl) - \langle I(hkl)\rangle| / \sum_{hkl}\sum_i I_i(hkl)$, where $I_i(hkl)$ is the intensity of a reflection, $\langle I(hkl)\rangle$ is the mean intensity of all i symmetry-related reflections and $N(hkl)$ is the multiplicity (Weiss, 2001). § Taken from *PHENIX* (Adams *et al.*, 2010); R_{free} is calculated using 5% of the total reflections that were randomly selected and excluded from refinement. ¶ DPI = $[N_{atoms}/(N_{refl} - N_{params})]^{1/2} RD_{max}C^{-1/3}$, where N_{atoms} is the number of atoms included in refinement, N_{refl} is the number of reflections included in refinement, R is the R factor, D_{max} is the maximum resolution of reflections included in refinement and C is the completeness of the observed data; for isotropic refinement, $N_{params} \simeq 4N_{atoms}$ (Cruickshank, 1999). †† Taken from *BAVERAGE* (Winn *et al.*, 2011). ‡‡ Taken from *PROCHECK* (Winn *et al.*, 2011).

cryoprotection buffer (0.1 *M* Bis-tris pH 6.5, 30% PEG 3350 and no glycerol) prior to cooling to 100 K.

2.8. Data collection and processing for native Acd_{DPN7} and for Acd_{DPN7} soaked with succinyl-CoA

Crystallographic data were collected using synchrotron radiation on the EMBL P13 beamline at the PETRA III storage ring, c/o Deutsches Elektronen Synchrotron (DESY), Hamburg, Germany. Crystals were cooled at 100 K with a cold nitrogen stream. The data were processed with *XDS* (Kabsch, 2010) and *AIMLESS* (Evans, 2006). Crystals of the apo form of the enzyme diffracted to 1.89 Å resolution and belonged to space group $P2_12_12$ with two monomers in the asymmetric unit and with unit-cell parameters a = 75.6, b = 100.6, c = 118.5 Å.

The structure was solved using the automated crystal structure-determination pipeline *Auto-Rickshaw* (Panjikar *et al.*, 2005) by molecular replacement using *BALBES* (Winn *et al.*, 2011) with the crystal structure of an acyl-CoA dehydrogenase from *Thermus thermophilus* HB8 (PDB entry 1ukw; RIKEN Structural Genomics/Proteomics Initiative, unpublished work) as the search model. The structure was refined using *ARP/wARP* v.7.1 (Perrakis *et al.*, 1999), *Coot* (Emsley *et al.*, 2010) and *PHENIX* (Adams *et al.*, 2010) to an R factor and R_{free} (5% of data) of 16.2 and 20.1%, respectively. Data-collection and refinement statistics are reported in Table 1.

The crystals of the complex of Acd_{DPN7} with the substrate analogue diffracted to 2.30 Å resolution and belonged to space group $P2_12_12$ with six monomers in the asymmetric unit and with unit-cell parameters a = 100.0, b = 233.4, c = 121.2 Å . The structure was solved by molecular replacement using *Phaser* (McCoy *et al.*, 2007) with monomer *A* of the native Acd_{DPN7} as the search model. Refinement progressed using *Coot* (Emsley *et al.*, 2010) and *PHENIX* (Adams *et al.*, 2010) to an R factor and R_{free} (5% of data) of 19.9 and 24.4%, respectively. Data-collection and refinement statistics are reported in Table 1.

3. Results and discussion

3.1. The crystal structure of apo Acd_{DPN7}

The crystal structure of 3-sulfinopropionyl-coenzyme A (3SP-CoA) desulfinase (Acd_{DPN7}) from *A. mimigardefordensis* was solved by molecular replacement using the monomer of an acyl-CoA dehydrogenase (Acd) from *T. thermophilus* HB8, which shares 36% sequence identity (PDB entry 1ukw; RIKEN Structural Genomics/Proteomics Initiative, unpublished work), as a search model.

Size-exclusion chromatography confirmed a native molecular mass of approximately 150–200 kDa (data not shown) as determined previously (Schürmann *et al.*, 2013) and corresponding to the tetrameric structure that was observed (Fig. 2*a*). The buried surface area and the free dissociation energy, calculated using *PISA* (Krissinel & Henrick, 2007), are 7583 Å^2 and 29.2 kcal mol^{-1} for the dimer and 23 211 Å^2 and 58.7 kcal mol^{-1} for the tetramer, respectively.

The overall fold of Acd_{DPN7} is similar to those previously determined for other Acds (Kim *et al.*, 1993; Thorpe & Kim, 1995; Fu *et al.*, 2004; Kim & Miura, 2004). The monomer consists of three regions: an initial N-terminal α-helical domain (helices A–F), a β-sheet domain (β-strands 1–7) and a second C-terminal α-helical domain (helices G–K) (Supplementary Table S2). The r.m.s. deviations between the C$^\alpha$ atoms of Acd_{DPN7} monomers *A* and *B* against monomer *A* of the Acd from *T. thermophilus* HB8 (PDB entry 1ukw) were 1.4 and 1.3 Å, respectively, as calculated using *Coot* (Emsley *et al.*, 2010) over 379 residues. These r.m.s.d. values are comparable

to those previously reported between other Acds (Fu *et al.*, 2004). Several amino-acid residues of Acd_{DPN7} are conserved throughout the entire Acd superfamily and are involved in FAD binding, *i.e.* the K-*X*-W/F-I-T motif (corresponding to KYWIT, residues 218–223, in Acd_{DPN7}; Kim *et al.*, 1993) and a G*XX*G motif (corresponding to GSSG, residues 342–345, in Acd_{DPN7}; Urano *et al.*, 2010).

Each FAD (Fig. 2*b*) is positioned with the riboflavin group close to the middle of β-strand 1 and the end of β-strand 3 of the first monomer and the adenine groups held between α-helices G and H of the second monomer. The flavin group forms an extended hydrogen-bond network with the side chains of Ser124(*A*) and Thr156(*A*) and the main chains of Ile121(*A*), Ile123(*A*), Ser124(*A*), Trp154(*A*) and Thr156(*A*) and two water molecules. These two regions correspond to the TEP*XX*GS and the K*X*W/FIT sequence motifs typically found in other Acds (Kim *et al.*, 1993; Bross *et al.*, 1990; Ye *et al.*, 2004). The dimethylbenzene portion of the FAD isoalloxazine ring is packed between Trp154(*A*) on one side and Ala365(*A*) on the other side to make the pocket more hydrophobic. In the active sites of both monomers one molecule of glycerol is present above the FAD isoalloxazine ring (Fig. 2*b*).

The ribitol group is tethered by hydrogen bonds to the side chain of Ser343(*B*), part of the G*XX*G motif (Urano *et al.*, 2010) and several waters. The pyrophosphate moiety interacts with the side chains of Ser130(*A*) and Arg272(*B*) and with local waters. The adenine group forms hydrogen bonds to the side chains of Thr368(*A*), Gln370(*A*), Gln387(*A*) and Gln339(*B*). Several hydrophobic residues are present such as Phe275(*B*), Phe282(*B*), Leu285(*B*) and Leu279(*B*).

The free dissociation energy, calculated using *PISA* (Krissinel & Henrick, 2007), for the dimer is 29.2 kcal mol^{-1}, while the free dissociation energy for the dimer depleted of the two FAD molecules is 17.6 kcal mol^{-1}, conferring a structural role on the FADs within the homodimeric structure.

3.2. Overall sequence and fold similarities of Acd_{DPN7} 3SP-CoA desulfinase to dehydrogenases

The 3SP-CoA desulfinase Acd_{DPN7} shares high structural similarity with acyl-CoA dehydrogenases and possesses one FAD per subunit. Thus, it is not structurally related to any of the previously reported desulfinases (Nakayama *et al.*, 2002; Lee *et al.*, 2006; Fernandez *et al.*, 2012). The average r.m.s.d. of Acd_{DPN7} monomer *A* against the coordinates of several other acyl-CoA dehydrogenases is ∼1.5 Å, as calculated by the *PDBeFold* v.2.56 server (Krissinel & Henrick, 2004; http://www.ebi.ac.uk/msd-srv/ssm/; Table 2). Acd_{DPN7} has evolved into a desulfinase while conserving 38% of the amino-acid residues common to the acyl-CoA dehydrogenase superfamily. For acyl-CoA dehydrogenases to have dehydrogenase activity, it is essential to have a catalytic base (Glu or Asp residue) at either position 246 or 366 (Schürmann *et al.*, 2013, 2014). In Acd_{DPN7} a glutamate is not found in either position: a glutamine residue is found at position 246 and a glycine residue is found at position 366. The absence of a Glu residue at either position 246 or 366 explains why Acd_{DPN7} and the other recently identified desulfinases (Schürmann *et al.*, 2014) are unable to catalyze the dehydrogenation of any tested acyl-CoA substrates. The most recurrent residues in acyl-CoA dehydrogenases corresponding to Gln246 in Acd_{DPN7} are Gly (seven occurences), Thr (four), Ala (three) and Glu (two) (Table 2). In the position corresponding to Gly366 in Acd_{DPN7}, the most recurrent residues found are Glu (14 occurrences) and Ala (two) (Table 2). Both the Gly366Glu and Gly366Ala mutations can be interpreted as the result of a single-nucleotide exchange in

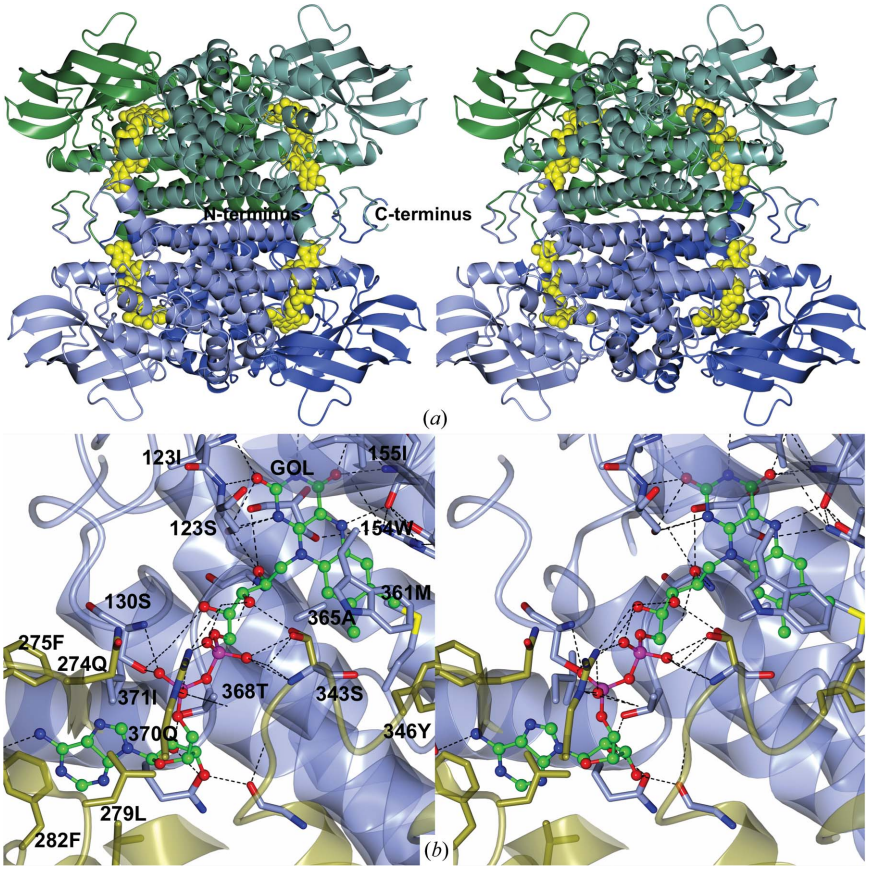

Figure 2
(*a*) Stereoview of the structure of 3-sulfinopropionyl-coenzyme A (3SP-CoA) desulfinase from *A. mimigardefordensis* strain DPN7^{T}. The two dimers that make up the tetramer are depicted in green and blue. Monomers of the dimers are depicted in the respective light or dark colour. The FAD molecules are depicted in a yellow space-filling representation. (*b*) The FAD molecule (ball-and-stick representation; carbon, green; oxygen, red; blue, nitrogen) is shared within the two monomers *A* (light blue) and *B* (gold). Amino-acid residues and a glycerol molecule (GOL) are depicted with fat bonds in light blue (monomer *A*) or gold (monomer *B*), with oxygen in red and nitrogen in blue.

Table 2
Three-dimensional alignment of Acd_{DPN7} with deposited dehydrogenases using *PDBeFold* (Krissinel & Henrick, 2004).

PDB code	R.m.s.d. (Å)	Sequence identity (%)	Position 1	Position 2	Position 3	Activity	Source	Reference
5af7	n/a	n/a	Arg84	Gln246	Gly366	3SP-CoA desulfinase	*Advenella mimigardefordensis*	This work
1jqi	1.156	33	Val90	Gly247	Glu368	Short-chain acyl-CoA dehydrogenase	*Rattus norvegicus*	Battaile *et al.* (2002)
3pfd	1.272	38	Leu95	Thr251	Glu373	Acyl-CoA dehydrogenase	*Mycobacterium thermoresistibile*	Abendroth *et al.* (2011)
2jif	1.293	33	Val137	Gly293	Glu414	Short branched-chain acyl-CoA dehydrogenase	*Homo sapiens*	A. C. W. Pike *et al.* (unpublished work)
1rx0	1.320	32	Ala99	Gly254	Glu376	Isobutyryl-CoA dehydrogenase	*Homo sapiens*	Battaile *et al.* (2004)
4kto	1.321	30	Leu90	Glu247	Ala368	Putative isovaleryl-CoA dehydrogenase	*Sinorhizobium meliloti*	New York Structural Genomics Research Consortium (unpublished work)
2dvl	1.323	34	Val83	Gly235	Glu356	Uncharacterized	*Thermus thermophilus*	RIKEN Structural Genomics/Proteomics Initiative (unpublished work)
3mdd	1.333	33	Thr96	Thr255	Glu376	Medium-chain acyl-CoA dehydrogenase	*Sus scrofa*	Kim *et al.* (1993)
4n5f	1.347	34	Thr85	Gly242	Glu363	Putative acyl-CoA dehydrogenase	*Burkholderia cenocepacia* J2315	Seattle Structural Genomics Center for Infectious Disease (unpublished work)
1ws9	1.348	35	Leu87	Gly248	Glu369	Uncharacterized	*Thermus thermophilus* HB8	RIKEN Structural Genomics/Proteomics Initiative (unpublished work)
1ivh	1.365	32	leu95	Glu254	Ala375	Isovaleryl-CoA dehydrogenase	*Homo sapiens*	Tiffany *et al.* (1997)
1buc	1.371	33	Ile88	Gly246	Glu367	Butyryl-CoA dehydrogenase	*Megasphaera elsdenii*	Djordjevic *et al.* (1995)
1ukw	1.418	36	Thr116	Thr272	Glu393	Medium-chain acyl-CoA dehydrogenase	*Thermus thermophilus* HB8	RIKEN Structural Genomics/Proteomics Initiative (unpublished work)
3mpi	1.507	29	Val88	Thr245	Glu367	Glutaryl-CoA dehydrogenase	*Desulfococcus multivorans*	Wischgoll *et al.* (2010)
1sir	1.550	22	Ser95	Ala249	Glu370	Glutaryl-CoA dehydrogenase	*Homo sapiens*	Fu *et al.* (2004)
3swo	1.553	22	Ser103	Ala254	Glu375	Glutaryl-CoA dehydrogenase	*Mycobacterium smegmatis*	Baugh *et al.* (2015)
3eom	1.668	20	Ser98	Ala253	Glu374	Glutaryl-CoA dehydrogenase	*Burkholderia pseudomallei*	Begley *et al.* (2011)

the DNA sequence from glutamate, *i.e.* GAA/GAG (Glu) to GGA (Gly) or GCA/GCG (Ala).

3.3. Identification and characterization of the active site

Superimposition of the structures of the glutaryl-CoA dehydrogenase from *Desulfococcus multivorans* in complex with glutaryl-CoA (PDB entry 3mpi; Wischgoll *et al.*, 2010) and of the medium-chain acyl-CoA dehydrogenase from pig liver mitochondria in complex with octanoyl-CoA (PDB entry 3mde; Kim *et al.*, 1993) with the structure of Acd_{DPN7} 3SP-CoA desulfinase indicates the cavity around the residues Arg84, Asp88, Lys118–Ile121, Tyr243–Gln246 and the isoalloxazine ring of FAD as the likely reaction centre of the Acd_{DPN7} 3SP-CoA desulfinase. To validate this hypothesis, Acd_{DPN7} was crystallized in the presence of succinyl-CoA, which represents a structural analogue of 3-sulfinopropionyl-CoA (3SP-CoA). The C atoms of the succinyl moiety are numbered 1–4, with position 4 corresponding to the terminal carboxylate. In 3SP-CoA position 4 corresponds to the terminal sulfino group (Fig. 3). Co-crystallization, followed by soaking with succinyl-CoA, resulted in the hydrolysis of succinyl–CoA. As reported by Wischgoll *et al.* (2010), suppression of the hydrolysis of the CoA thioesters of dicarboxylic acids was the major challenge in co-crystallization, as the electron density calculated from most data sets for glutaryl-CoA dehydrogenases co-crystallized in the presence of 5 m*M* glutaryl-CoA solely contained CoA.

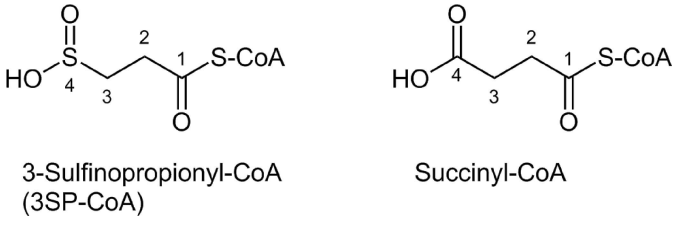

Figure 3
Chemical representation of 3-sulfinopropionyl-coenzyme A (3SP-CoA) and its substrate analogue succinyl-coenzyme A.

In the active sites of Acd_{DPN7} monomers *A*, *B*, *D*, *E* and *F* only the CoA group could be observed based on the electron-density maps (Fig. 4 and Supplementary Fig. S1). For monomer *C* no electron density was observed that could be related to a CoA group, but a succinyl group was modelled at the deep end of the cavity. The $F_o - F_c$ difference Fourier OMIT maps, calculated without the substrate at a 3.0σ contour level (Fig. 4 and Supplementary Fig. S1), mark the positions of the adenosine group, the ribitol group, the three phosphoryl groups, the carbonyl group of the pantothenic moiety and the CoA S atom, thus guiding the positioning of the entire CoA group. The real-space correlation coefficients computed by *PHENIX* (Adams *et al.*, 2010) for the CoA group bound in monomers *A*, *B*, *D*, *E* and *F* are 0.7, 0.81, 0.73, 0.77 and 0.75, respectively. The correlation factors with the $2F_o - F_c$ map calculated using *OVERLAPMAP* (Winn *et al.*, 2011) are 0.50 (0.66), 0.57 (0.70), 0.54 (0.63), 0.57 (0.69) and 0.59 (0.75), respectively. The values in parentheses are the correlation factors with the $2F_o - F_c$ feature-enhanced map (Pražnikar *et al.*, 2009; Afonine *et al.*, 2015; Fig. 4 and Supplementary Fig. S1). We refined the occupancies of the five CoA groups to obtain *B*-factor values close to those observed for the surrounding protein residues. The final occupancy values for

the CoA groups of monomers *A*, *B*, *D*, *E* and *F* were 0.43 (57 Å^2), 0.48 (61 Å^2), 0.57 (60 Å^2), 0.53 (67 Å^2) and 0.59 (72 Å^2), respectively (the *B*-factor values are given in parentheses). Cruickshank's DPI for coordinate error based on the *R* factor (Cruickshank, 1999) for the complete structure is 0.3 Å, including the refined CoA groups. No electron density reminiscent of the presence of PEG, which was used for crystallization and cryoprotection of both the native enzyme and of the complex, was observed in the crystal structure of the apoenzyme, therefore its presence was also excluded in the active site of the structure of the complex. Moreover, no glycerol was used for crystallization or cryoprotection of the complex, since its presence was observed in the active site of the native enzyme above the FAD isoalloxazine ring. At the deep end of the active sites of the complex structure only a few waters were observed at a contour level of 1.0σ in $2F_o - F_c$ Fourier maps. The positioning of the CoA groups within the Acd_{DPN7} cavity is consistent across the monomers (Supplementary Fig. S2), thus allowing identification of the active site of the enzyme.

The adenosine group of CoA is at a hydrogen-bonding distance from the side chains of Asn244 and Arg247. In particular, the OD1 atom of Asn244 is 2.9 Å from the N6A atom of the adenosine group, while the ND2 atom of Asn244 is at 3.2 Å from the N1A atom of the adenosine group (the values reported are for monomer *D*, with similar values for the remaining monomers). Arg247 is involved in proper positioning of the CoA moiety (Erb *et al.*, 2009; Kim *et al.*, 1993) as observed in our structure. In other structures of acyl-CoA dehydrogenases the arginine residues corresponding to Arg247 are strictly conserved (Fu *et al.*, 2004). In most cases they interact with the two carbonyl O atoms of the amide groups of CoA (Arg248 in PDB entry 1jqi, Arg255 in PDB entry 1rx0, Arg246 in PDB entry 3mpi and Arg256 in PDB entry 1udy). In medium-chain acyl-CoA dehydrogenases (MCADs; PDB entry 1udy; Satoh *et al.*, 2003), there are two Arg residues interacting with the CoA moiety, which are Arg324 (interacting with the CoA adenine ring) and Arg256 (interacting with a carbonyl O atom). In Acd_{DPN7} there is no equivalent of Arg324 in MCAD, and Arg247 (corresponding

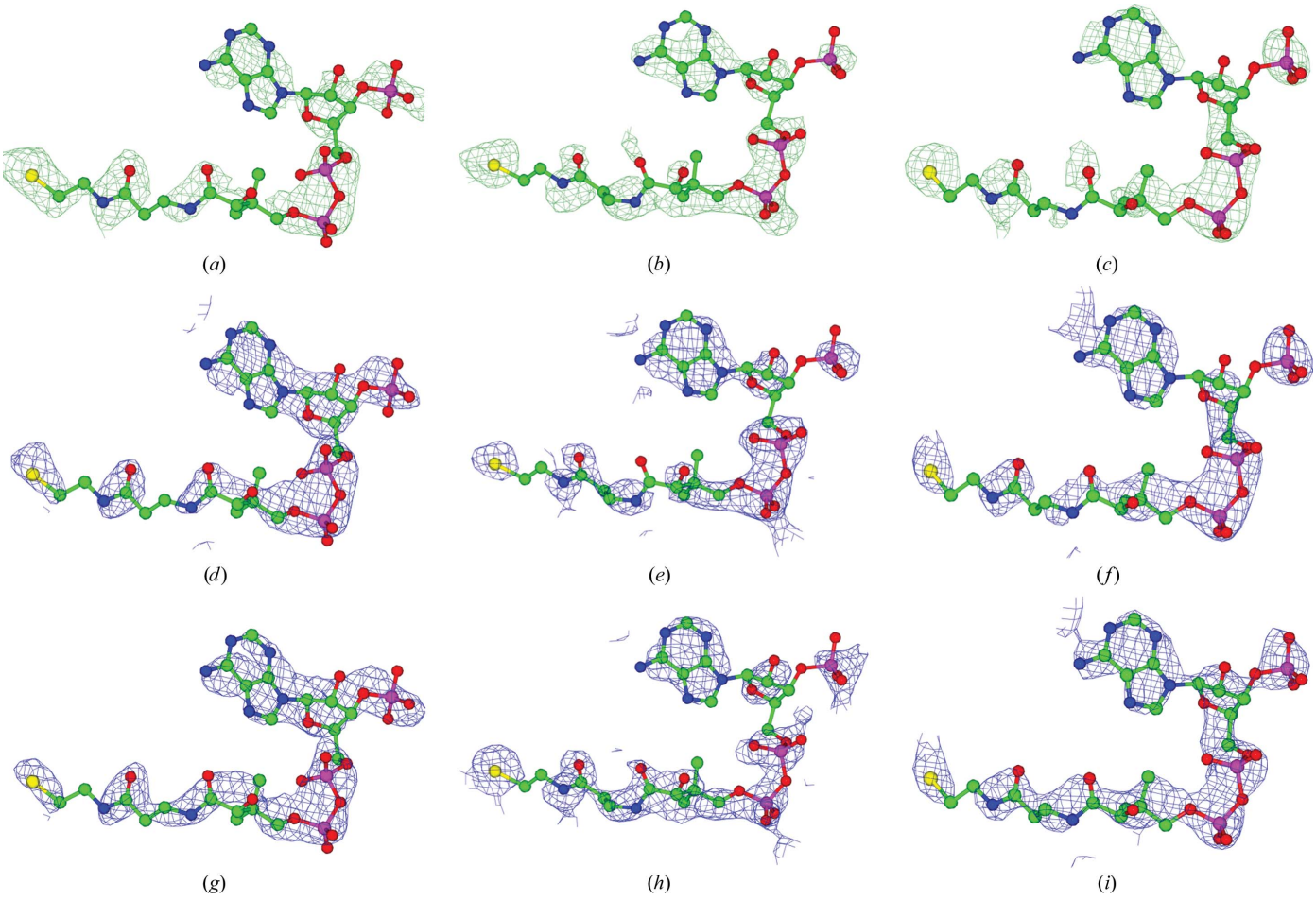

Figure 4
The coenzyme A groups of monomers *B* (*a*, *d*, *g*), *D* (*b*, *e*, *h*) and *F* (*c*, *f*, *i*) depicted in ball-and-stick representation (with atoms colour-coded as follows: carbon, green; oxygen, red; phosphorus, magenta; nitrogen, blue; sulfur, yellow) fitted into (top row) $F_o - F_c$ difference Fourier OMIT maps (green mesh; contour level 3.0σ, calculated without the substrate), (middle row) $2F_o - F_c$ difference Fourier maps (blue mesh; contour level 1.0σ) calculated with *PHENIX* (Adams *et al.*, 2010) and (bottom row) $2F_o - F_c$ difference Fourier maps (blue mesh; contour level 2.0σ) using the 'feature-enhanced' option of *PHENIX* (Adams *et al.*, 2010; Pražnikar *et al.*, 2009; Afonine *et al.*, 2015).

to Arg256 in MCAD) is close to both the carbonyl O atom and the adenine ring of CoA. Arg247 might have a role in recognition of the adenosine group. An Arg250Trp mutation (corresponding to Arg247 in Acd_{DPN7}) was found to be pathogenic in human glutaryl-CoA DH (Schwartz *et al.*, 1998).

The three phosphoryl groups of the CoA are at 3.1 Å from Lys384 and tether a network of waters. Several hydrophobic residues (Phe236, Met240 and Ile316) define the entrance to the substrate-binding pocket. The NH group of the pantothenic moiety of CoA forms a hydrogen bond to the carbonyl group of the main chain of Ser130 at 2.7 Å. The Arg247 side chain is placed between the carbonyl groups within the pantothenic moiety of CoA. The CoA S atom sits above the planar flavin group at a distance of 3.1 Å from it and at 3.4 Å from the Tyr243 OH group. The presence of Tyr243 increases the polarity of the cavity compared with other Acds, where a phenylalanine or leucine is normally found in the corresponding position.

The unit-cell contents of the apo form and the analogue-complex crystal were different, with one dimer in the apo form and three dimers in the complex structure. Both crystals belonged to the same space group ($P2_12_12$) and have the same Matthews coefficient (Table 1). Their unit-cell dimensions are related by a (0, 1, 0; 3, 0, 0; 0, 0, 1) transformation matrix. In lattices, these changes generally occur because of differences in cryoprotection, cooling and/or soaking with compounds that bind into the crystal and potentially distort the lattice to the extent that there are changes in the unit-cell parameters and space group. In this case, the addition of fresh succinyl-CoA and the omission of glycerol from the cryo-conditions might have caused the rearrangement of the unit cell of the soaked crystal. Superimposition of the C^{α} atoms of Acd_{DPN7} monomer *A* (residues 2–392) in the apo form and monomers of the complex with CoA shows r.m.s. deviations (of >1 Å) only for residues Gly143, Asp173 and Gly190 in external loops. The r.m.s. deviation of Acd_{DPN7} monomer *A* and each monomer of the complex with CoA, calculated over the C^{α} atoms of residues 2–392, is <0.5 Å.

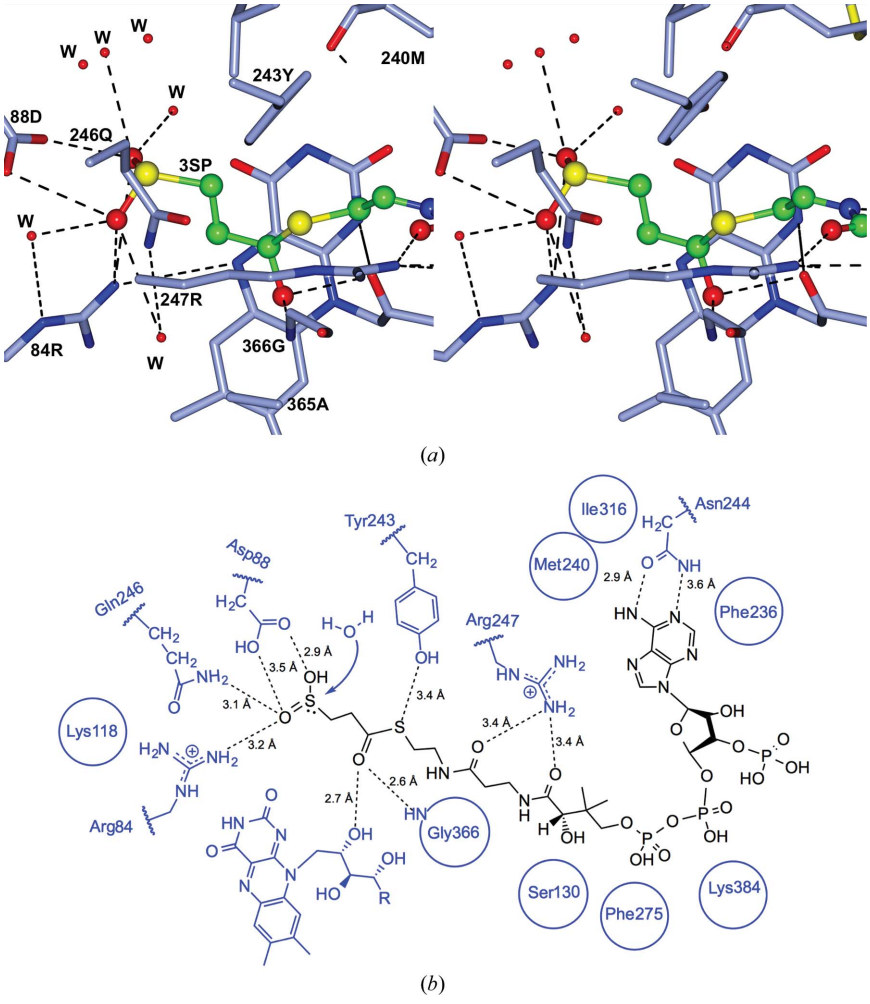

Figure 5
Views of the positioning of the 3SP-CoA group within the active site of Acd_{DPN7} (3SP-CoA desulfinase) from *A. mimigardefordensis* after molecular-dynamics minimization. 3SP-CoA was positioned on the basis of the crystallographically refined positions of CoA within the cavity of 3SP-CoA desulfinase. (*a*) Stereoview of the deep end of the cavity. 3SP-CoA is depicted in ball-and-stick representation with atoms colour-coded as follows: carbon, green; oxygen, red; nitrogen, blue; sulfur, yellow). The protein is depicted with fat bonds in cyan, with O atoms in red and N atoms in blue. Waters (W) are depicted as red spheres. (*b*) Two-dimensional representation of the entire binding site.

3.4. Modelling of 3SP-CoA within Acd_{DPN7} 3SP-CoA desulfinase

Superimposition of the structures of the glutaryl-CoA dehydrogenase from *D. multivorans* in complex with glutaryl-CoA (PDB entry 3mpi; Wischgoll *et al.*, 2010) and of the medium-chain acyl-CoA dehydrogenase from pig liver mitochondria in complex with octanoyl-CoA (PDB entry 3mde; Kim *et al.*, 1993) with the structure of Acd_{DPN7} 3SP-CoA desulfinase in complex with a CoA group confirms that the binding of glutaryl-CoA and octanoyl-CoA to the respective dehydrogenases shares the same binding pattern as that for CoA within the Acd_{DPN7} cavity (Supplementary Fig. S3).

In order to investigate which residues in the active site might interact with the terminal sulfino group of the substrate, 3SP-CoA was modelled on the structure of the bound CoA moiety (Fig. 5*a*). A round of molecular dynamics (*phenix.dynamics*) was then performed on the model with default settings in order to de-bias the model and obtain the correct geometry (Adams *et al.*, 2010).

This clearly shows the propionyl group (C-atom positions 1–3; Fig. 3) placed with the S atom (position 4) of the sulfino group within 3.5 Å distance of the side chains of Arg84, Asp88 and Gln246 above the plane

Table 3
3SP-CoA desulfination activity of Acd_{DPN7} mutants.

ND, not determined.

Acd_{DPN7}	K_m (mM)	Specific activity (μmol min^{-1} mg^{-1})	k_{cat} (s^{-1})	k_{cat}/K_m (s^{-1}mM^{-1})
Wild type (Schürmann *et al.*, 2013)	0.013 ± 0.001†	4.19 ± 0.07†	3.13 ± 0.05†	237.2 ± 4.1†
R84K	ND	0.00 ± 0.00‡	0.00 ± 0.00‡	ND
Q246E	0.019 ± 0.000	5.26 ± 0.05	3.93 ± 0.04	203.2 ± 1.9

† Standard deviations which were not given in the original publication were recalculated based on the raw data. The k_{cat}/K_m value reported here differs from the original value owing to rounding errors in the original publication which are now omitted. ‡ No enzyme activity was observed even when the purified enzyme was applied at 65 μg ml^{-1}, while 2 μg ml^{-1} enzyme was applied in the assays with the wild-type enzyme and the Acd_{Q246E} mutant. Measurements were performed in triplicate.

of the isoalloxazine ring of FAD (Figs. 5*a* and 5*b*). A network of waters can be accommodated within hydrogen-bonding distance of the sulfino group (Fig. 5*a*).

In this model the carbonyl O atom of the 3SP-CoA thioester linkage is hydrogen-bonded both to the 2′-OH of the ribityl side chain of FAD and to the main-chain NH of Gly366. In general, in acyl-CoA dehydrogenases the carbonyl O atom of the thioester linkage of the substrate is hydrogen-bonded both to the 2′-OH of the ribityl side chain of FAD and to the main-chain NH of Glu376 (Kim *et al.*, 1993). These interactions are important in the orientation and polarization of the carbonyl group of the substrate (Kim *et al.*, 1993; Thorpe & Kim, 1995). In the dehydrogenase case, polarization of the substrate carbonyl group is necessary to lower the pK_a value of the α-carbon of the substrate, which is necessary for the dehydrogenation reaction. It still remains to be understood whether this polarization effect is also important in the desulfination reaction of 3SP-CoA.

The Arg84, Asp88 and Gln246 side chains and the isoalloxazine ring of FAD thus define the enzymatic environment for the desulfination reaction. The distance of 3SP-CoA S4 from the isoalloxazine ring of FAD would be >3.8 Å.

3.5. The mutant enzymes Acd_{DPN7_R84K} and Acd_{DPN7_Q246E}

Modelling of 3SP-CoA within the Acd_{DPN7} 3SP-CoA desulfinase active site positions the sulfino group close to Arg84, with an Arg84 NH2–3SP-CoA OS5 distance of 3.2 Å (Fig. 5*b*). Residue Arg84 has been proposed to be involved in binding of the sulfino group of 3SP-CoA, as a similar interaction was observed in glutaryl-CoA dehydrogenases (Schürmann *et al.*, 2013). In these enzymes, an arginine residue is involved in binding the terminal carboxyl group (Schaarschmidt *et al.*, 2011; Dwyer *et al.*, 2000, 2001; Wischgoll *et al.*, 2009, 2010). To investigate whether this residue is essential for the desulfination reaction, Arg84 was mutated to lysine in an Acd_{DPN7_R84K} variant. Size-exclusion chromatography of wild-type Acd_{DPN7} and Acd_{DPN7_R84K} illustrates that Acd_{DPN7_R84K} was purified as an intact tetramer and hence as a folded protein. The absorption spectrum of Acd_{DPN7_R84K} is identical to the spectrum of Acd_{DPN7} published by Schürmann *et al.* (2013) (Supplementary Fig. S4). This indicates that all FAD binding sites are saturated and that the tetramer is properly folded. Mutation of Arg84 to Lys resulted in complete loss of activity (Table 3), indicating an essential role of Arg84. Sulfinic acids are more acidic than their carboxylic acid counterparts (Fujihara & Furukawa, 1990) and thus are deprotonated at physiological pH. The guanidinium group of Arg84 has a pK_a of 12.5 and is expected to be positively charged at physiological pH, hence stabilizing the negatively charged sulfino group. Given the similar pK_a of the amino and guanidinium groups (11 and 12.5, respectively, for Lys and Arg), the two side chains would both be expected to be protonated at physiological pH and should both be able to stabilize the negatively charged sulfino group. Arg84 would bear a positive charge delocalized over the guanidinium group (Rozas *et al.*, 2013; Neves *et al.*, 2012), while a lysine would bear a very localized positive charge on the NZ atom. Hence, stabilization of the charge could be only one aspect of the role of the Arg84 side chain. In addition, the guanidinium cation is a strong hydrogen-bond donor (Neves *et al.*, 2012).

In the model, the Gln246 NE2–3SP-CoA OS5 distance is 3.1 Å (Fig. 5*b*) and it was previously postulated that the presence of Gln246 would be responsible for the inability of Acd_{DPN7} to catalyze an acyl-CoA dehydrogenase reaction (Schürmann *et al.*, 2013). Thus, an Acd_{DPN7_Q246E} variant was generated. This variant was still able to act as a desulfinase (Table 3), but could not utilize any of the tested acyl-CoA dehydrogenase substrates propionyl-CoA, butyryl-CoA, isobutyryl-CoA, valeryl-CoA, isovaleryl-CoA, succinyl-CoA, glutaryl-CoA and 3SP-CoA (results not shown). Consequently, the Acd_{DPN7_Q246E} mutant did not gain acyl-CoA dehydrogenase activity upon the mutation of the glutamine to a glutamate. However, in the Acd_{DPN7_Q246E} mutant the substitution has a slight effect on the desulfination rate (Table 3). The K_m increases by about 46%, while the k_{cat} value increases by about 25%, from the wild type to the mutant. Substrate binding appears to be partially impaired, probably owing to the newly added negatively charged carboxylic group (mutation of glutamine to glutamate), which might repel the entrance of the negatively charged 3-sulfinopropionyl group. The reaction rate is presumably enhanced by a more negatively charged cavity, which would help in removal of the HSO_3^- group upon desulfination.

3.6. The reaction mechanism

The desulfination reaction of Acd_{DPN7} was described as being independent of an artificial electron acceptor (Schürmann *et al.*, 2013). Hence, this indicated that FAD is not involved in electron transfer during the reaction. Nonetheless, the possibility that oxygen may serve as an electron acceptor could not be excluded in the previous study as the reactions

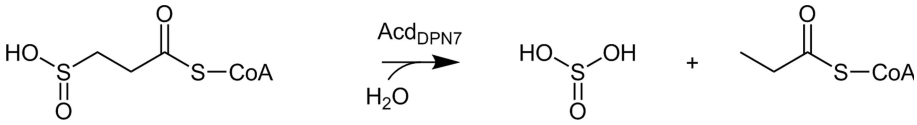

Figure 6
General reaction mechanism of the 3SP-CoA desulfinase Acd$_{DPN7}$ from *A. mimigardefordensis* DPN7^T.

were performed under aerobic conditions. Thus, the oxygen-dependency of Acd$_{DPN7}$ was further investigated as described in §2. Acd$_{DPN7}$ showed no significant difference in reaction velocity in the presence or absence of O_2 (Supplementary Fig. S5). Furthermore, the oxygen content of the reaction mixture was assayed using an oxygen micro-respiration sensor and clearly showed that no O_2 was consumed during the desulfination reaction (Supplementary Fig. S5). These results confirmed that oxygen does not serve as an electron acceptor during the reaction of Acd$_{DPN7}$. Together with the results from a previous study (Schürmann *et al.*, 2013), it can be concluded that FAD (fully oxidized form or semiquinone form) is not reduced to FADH$_2$ (hydroquinone form) during the desulfination reaction, which would require a subsequent electron transfer to regenerate FAD. In fact, Acd$_{DPN7}$ could still catalyze the desulfination reaction when the FAD cofactor was reduced to FADH$_2$ (Supplementary Fig. S6). After reduction of the cofactor with dithionite, Acd$_{DPN7}$ (containing FADH$_2$) showed about 76% of the activity of Acd$_{DPN7}$ (Supplementary Fig. S6). Some flavoenzymes catalyze reactions with no net redox change, in which the flavin, acting either as an electron donor and nucleophile or as a base, modulates the reactivity of the protein environment to perform novel reactions (Sobrado, 2012). In the reaction catalyzed by chorismate synthase, the flavin might act as a base/H-atom abstractor for C—H bond cleavage after breakage of the C—O bond (Osborne *et al.*, 2000). In UDP-galactopyranose mutase, the flavin acts as a nucleophile attacking the anomeric C atom of galactose (Soltero-Higgin *et al.*, 2004). In contrast, type II isopentenyl diphosphate isomerase employs novel dual flavin functionalities, in which it acts both as an acid and as a base (Unno *et al.*, 2009). In alkyl-dihydroxyacetonephosphate synthase (Razeto *et al.*, 2007) and UDP-galactopyranose mutase (Soltero-Higgin *et al.*, 2004) the flavin cofactor acts as a molecular scaffold to hold the intermediate during catalysis to permit interaction with a second substrate. The reduction in activity by 24% of the reduced form *versus* the oxidized form is significant and may point to a mechanism where, in the case of Acd$_{DPN7}$, the N5 atom of FAD might act as a weak base either for the hydrogen at position 3 of the 3-sulfinopropionyl group (positioned above N5), for the sulfinopropionyl group itself or for a water molecule to prepare a nucleophilic attack. The interactions between the CoA moiety and the FAD might also help in proper positioning of the substrate. The enzymatic reaction (Fig. 6) might progress with hydrogen-bond formation and charge transfer between the guanidinium cation of Arg84 and 3SP-CoA, which would favour nucleophilic attack of a water molecule on the S atom of the sulfino group. Hydrogen-bond formation and charge transfer between guanidine/guanidinium and anion complexes has been shown theoretically in aqueous solvation studies (Rozas *et al.*, 2013).

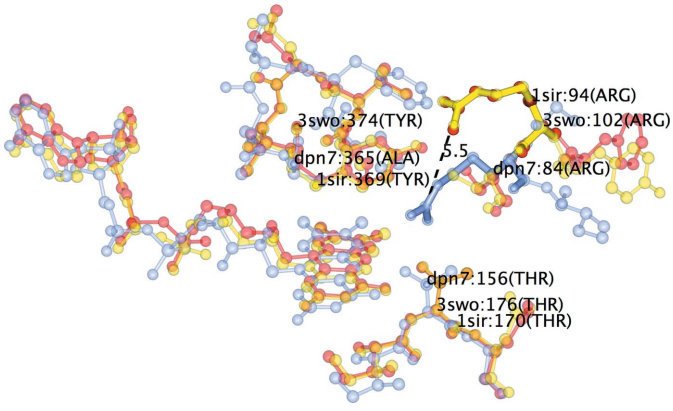

Figure 7
Superimposition of the active sites of human glutaryl-CoA dehydrogenase (PDB entry 1sir, yellow), *M. thermoresistible* glutaryl-CoA dehydrogenase (PDB entry 3swo, red) and the desulfinase Acd$_{DPN7}$ (cyan), showing Arg84 of Acd$_{DPN7}$ to be positioned within one residue of Arg94 of glutaryl-CoA dehydrogenase, *i.e.* 5.5 Å apart.

3.7. Evolution of acyl-CoA dehydrogenases into desulfinases

The mutant enzyme Acd$_{DPN7_R84K}$ completely loses its enzymatic activity (Table 3), indicating an essential role of Arg84 in catalysis. Furthermore, an arginine residue in a position corresponding to Arg84 in Acd$_{DPN7}$ is found in the primary sequence of each of the novel desulfinases (Schürmann *et al.*, 2014). In acyl-CoA dehydrogenases the most recurrent residues in the equivalent three-dimensional structure to position 84 of Acd$_{DPN7}$ are Thr (four instances), Val (three), Ser (three), Leu (two), Ala (one) and Ile (one) (Table 2). In Acd$_{DPN7}$ the codon found to code for Arg84 is CGA, making it plausible that a Leu residue (CTA) might have evolved into an Arg by another single-point mutation, thus relating desulfinases to isovaleryl-CoA dehydrogenases following a total of three point mutations (position 84, Leu to Arg; position 246, Glu to Gln; position 366, Ala to Gly). The three-dimensional structure comparison (Table 2) and the phylogenetic tree proposed for the desulfinases (Schürmann *et al.*, 2014) do indeed relate Acd$_{DPN7}$ to a *Homo sapiens* isovaleryl-CoA dehydrogenase (IVD; AAF20182.1; PDB entry 1ivh). It can be concluded that Acd$_{DPN7}$ became a desulfinase by losing the Glu residues from either position 246 or 366 and acquiring an Arg in position 84 as key modifications.

Acd$_{DPN7}$ Arg84 is spatially equivalent to Ser95 of human glutaryl-CoA dehydrogenase (Ser103 of *Mycobacterium thermoresistible* glutaryl-CoA dehydrogenase) as indicated by the three-dimensional alignment (Table 2). In position 94 of human glutaryl-CoA dehydrogenase (position 102 of

M. thermoresistible glutaryl-CoA dehydrogenase) an arginine is present, making the association with Acd_{DPN7} Arg84 plausible. The sequence alignment between the human and the *M. thermoresistible* glutaryl-CoA dehydrogenases and Acd_{DPN7} shows that this residue is shifted by one residue, *i.e.* it is not strictly conserved in the same primary position. Also spatially, Acd_{DPN7} Arg84 is found at ∼4 Å from the isoalloxazine ring of FAD, about 5.5 Å closer to the FAD than the conserved Arg residue in some glutaryl-CoA dehydrogenases (PDB entries 1sir or 3swo; Fig. 7), which is located ∼9.5 Å from the isoalloxazine ring of FAD. The different positioning of these two arginine residues within the dehydrogenase cavity can be accounted for as an adaptation to the different lengths of the non-CoA moieties of the substrates. The glutaryl moiety has five C atoms, while the sulfinopropionyl moiety has three C atoms plus one S atom. The same residue in two proximal positions appears to serve different enzymatic reactions (decarboxylation *versus* desulfination) within the same scaffold. In glutaryl-CoA dehydrogenases Arg94 does not make a major contribution to substrate binding, but its electric field could stabilize the reaction intermediates (Dwyer *et al.*, 2001; Schaarschmidt *et al.*, 2011). In human glutaryl-CoA dehydrogenase (PDB entry 1sir) Arg94Gly and Arg94Leu are pathogenic mutations (Goodman *et al.*, 1998; Zschocke *et al.*, 2000). In the desulfinase Acd_{DPN7} the guanidinium cation of Arg84 might function as a strong hydrogen-bond donor *via* the NH_2 and NH groups.

4. Conclusions

Acd_{DPN7} is the first desulfinase with an acyl-CoA dehydrogenase fold to be reported. The structures of native Acd_{DPN7} and of native Acd_{DPN7} soaked with succinyl-CoA as a structural substrate analogue show the interactions between the substrate and residues within the binding cavity, thus allowing a hypothesis on the mechanism of the desulfination reaction of this novel desulfinase enzyme with an acyl-CoA dehydrogenase scaffold to be formulated. Overall, the structural characterization of Acd_{DPN7} indicates the versatility of the acyl-CoA dehydrogenase scaffold to adapt to catalyze a new reaction as a desulfinase and expands our understanding of a bacterial desulfination pathway. These structural studies and biochemical data contribute to formulating a mechanistic proposal, which is by no means complete, but provides a basis for more extensive studies on this desulfination reaction.

Acknowledgements

We sincerely thank Johannes Nolte MSc for providing purified SucCD from *E. coli* BL21 (DE3). We thank Professor Maria A. Vanoni (University of Milan, Italy) for her valuable comments. This work was supported by the European Community's Seventh Framework Program under Contract 227764 P-Cube). The nucleotide sequence of Acd_{DPN7} is available under accession No. JX535522.1. We would like to thank the sample preparation and characterization facility (SPC) for assistance in crystallization and soaking experiments.

References

Abendroth, J., Gardberg, A. S., Robinson, J. I., Christensen, J. S., Staker, B. L., Myler, P. J., Stewart, L. J. & Edwards, T. E. (2011). *J. Struct. Funct. Genomics*, **12**, 83–95.
Adams, P. D. *et al.* (2010). *Acta Cryst.* D**66**, 213–221.
Afonine, P. V., Moriarty, N. W., Mustyakimov, M., Sobolev, O. V., Terwilliger, T. C., Turk, D., Urzhumtsev, A. & Adams, P. D. (2015). *Acta Cryst.* D**71**, 646–666.
Altschul, S. F., Madden, T. L., Schäffer, A. A., Zhang, J., Zhang, Z., Miller, W. & Lipman, D. J. (1997). *Nucleic Acids Res.* **25**, 3389–3402.
Battaile, K. P., Molin-Case, J., Paschke, R., Wang, M., Bennett, D., Vockley, J. & Kim, J.-J. P. (2002). *J. Biol. Chem.* **277**, 12200–12207.
Battaile, K. P., Nguyen, T. V., Vockley, J. & Kim, J.-J. P. (2004). *J. Biol. Chem.* **279**, 16526–16534.
Baugh, L. *et al.* (2015). *Tuberculosis (Edinb.)*. **95**, 142–148.
Begley, D. W., Davies, D. R., Hartley, R. C., Hewitt, S. N., Rychel, A. L., Myler, P. J., Van Voorhis, W. C., Staker, B. L. & Stewart, L. J. (2011). *Acta Cryst.* F**67**, 1060–1069.
Birnboim, H. C. & Doly, J. (1979). *Nucleic Acids Res.* **7**, 1513–1523.
Bradford, M. M. (1976). *Anal. Biochem.* **72**, 248–254.
Bross, P., Engst, S., Strauss, A. W., Kelly, D. P., Rasched, I. & Ghisla, S. (1990). *J. Biol. Chem.* **265**, 7116–7119.
Bruland, N., Wübbeler, J. H. & Steinbüchel, A. (2009). *J. Biol. Chem.* **284**, 660–672.
Cruickshank, D. W. J. (1999). *Acta Cryst.* D**55**, 583–601.
Djordjevic, S., Pace, C. P., Stankovich, M. T. & Kim, J.-J. P. (1995). *Biochemistry*, **34**, 2163–2171.
Dwyer, T. M., Rao, K. S., Goodman, S. I. & Frerman, F. E. (2000). *Biochemistry*, **39**, 11488–11499.
Dwyer, T. M., Rao, K. S., Westover, J. B., Kim, J.-J. P. & Frerman, F. E. (2001). *J. Biol. Chem.* **276**, 133–138.
Emsley, P., Lohkamp, B., Scott, W. G. & Cowtan, K. (2010). *Acta Cryst.* D**66**, 486–501.
Erb, T. J., Fuchs, G. & Alber, B. E. (2009). *Mol. Microbiol.* **73**, 992–1008.
Evans, P. (2006). *Acta Cryst.* D**62**, 72–82.
Fernandez, F. J., de Vries, D., Peña-Soler, E., Coll, M., Christen, P., Gehring, H. & Vega, M. C. (2012). *Biochim. Biophys. Acta*, **1824**, 339–349.
Fu, Z., Wang, M., Paschke, R., Rao, K. S., Frerman, F. E. & Kim, J.-J. P. (2004). *Biochemistry*, **43**, 9674–9684.
Fujihara, H. & Furukawa, N. (1990). *The Chemistry of Sulfinic Acids, Esters and Their Derivatives.*, edited by S. Patai, pp. 275–295. Chichester: John Wiley & Sons.
Goodman, S. I., Stein, D. E., Schlesinger, S., Christensen, E., Schwartz, M., Greenberg, C. R. & Elpeleg, O. N. (1998). *Hum. Mutat.* **12**, 141–144.
Jollés-Bergeret, B. (1974). *Eur. J. Biochem.* **42**, 349–353.
Kabsch, W. (2010). *Acta Cryst.* D**66**, 125–132.
Kim, J.-J. P. & Miura, R. (2004). *Eur. J. Biochem.* **271**, 483–493.
Kim, J.-J. P., Wang, M. & Paschke, R. (1993). *Proc. Natl Acad. Sci. USA*, **90**, 7523–7527.
Krissinel, E. & Henrick, K. (2004). *Acta Cryst.* D**60**, 2256–2268.
Krissinel, E. & Henrick, K. (2007). *J. Mol. Biol.* **372**, 774–797.
Lee, W. C., Ohshiro, T., Matsubara, T., Izumi, Y. & Tanokura, M. (2006). *J. Biol. Chem.* **281**, 32534–32539.
Lehman, T. C., Hale, D. E., Bhala, A. & Thorpe, C. (1990). *Anal. Biochem.* **186**, 280–284.
Leutwein, C. & Heider, J. (2002). *Arch. Microbiol.* **178**, 517–524.
Lütke-Eversloh, T. & Steinbüchel, A. (2003). *FEMS Microbiol. Lett.* **221**, 191–196.
McCoy, A. J., Grosse-Kunstleve, R. W., Adams, P. D., Winn, M. D., Storoni, L. C. & Read, R. J. (2007). *J. Appl. Cryst.* **40**, 658–674.

Mihara, H., Kurihara, T., Yoshimura, T., Soda, K. & Esaki, N. (1997). *J. Biol. Chem.* **272**, 22417–22424.
Nakayama, N., Matsubara, T., Ohshiro, T., Moroto, Y., Kawata, Y., Koizumi, K., Hirakawa, Y., Suzuki, M., Maruhashi, K., Izumi, Y. & Kurane, R. (2002). *Biochim. Biophys. Acta*, **1598**, 122–130.
Neves, M. A., Yeager, M. & Abagyan, R. (2012). *J. Phys. Chem. B*, **116**, 7006–7013.
Osborne, A., Thorneley, R. N., Abell, C. & Bornemann, S. (2000). *J. Biol. Chem.* **275**, 35825–35830.
Panjikar, S., Parthasarathy, V., Lamzin, V. S., Weiss, M. S. & Tucker, P. A. (2005). *Acta Cryst.* D**61**, 449–457.
Perrakis, A., Morris, R. & Lamzin, V. (1999). *Nature Struct. Biol.* **6**, 458–463.
Pražnikar, J., Afonine, P. V., Gunčar, G., Adams, P. D. & Turk, D. (2009). *Acta Cryst.* D**65**, 921–931.
Razeto, A., Mattiroli, F., Carpanelli, E., Aliverti, A., Pandini, V., Coda, A. & Mattevi, A. (2007). *Structure*, **15**, 683–692.
Riddles, P. W., Blakeley, R. L. & Zerner, B. (1983). *Methods Enzymol.* **91**, 49–60.
Rozas, I., Sánchez-Sanz, G., Alkorta, I. & Elguero, J. (2013). *J. Phys. Org. Chem.* **26**, 378–385.
Sadegh, C. & Schreck, R. P. (2003). *MIT Undergrad. Res. J.* **8**, 39–43.
Sambrook, J., Fritsch, E. F. & Maniatis, T. (1989). *Molecular Cloning: A Laboratory Manual*, 2nd ed. New York: Cold Spring Harbor Laboratory Press.
Satoh, A., Nakajima, Y., Miyahara, I., Hirotsu, K., Tanaka, T., Nishina, Y., Shiga, K., Tamaoki, H., Setoyama, C. & Miura, R. (2003). *J. Biochem.* **134**, 297–304.
Schaarschmidt, J., Wischgoll, S., Hofmann, H. J. & Boll, M. (2011). *FEBS Lett.* **585**, 1317–1321.
Schürmann, M., Demming, R. M., Krewing, M., Rose, J., Wübbeler, J. H. & Steinbüchel, A. (2014). *J. Bacteriol.* **196**, 882–893.
Schürmann, M., Deters, A., Wübbeler, J. H. & Steinbüchel, A. (2013). *J. Bacteriol.* **195**, 1538–1551.
Schürmann, M., Wübbeler, J. H., Grote, J. & Steinbüchel, A. (2011). *J. Bacteriol.* **193**, 3078–3089.
Schwartz, M., Christensen, E., Superti-Furga, A. & Brandt, N. J. (1998). *Hum. Genet.* **102**, 452–458.
Simon, E. J. & Shemin, D. (1953). *J. Am. Chem. Soc.* **75**, 2520
Sobrado, P. (2012). *Int. J. Mol. Sci.* **13**, 14219–14242.
Soltero-Higgin, M., Carlson, E. E., Gruber, T. D. & Kiessling, L. L. (2004). *Nature Struct. Mol. Biol.* **11**, 539–543.
Thorpe, C. & Kim, J.-J. P. (1995). *FASEB J.* **9**, 718–725.
Tiffany, K. A., Roberts, D. L., Wang, M., Paschke, R., Mohsen, A. W., Vockley, J. & Kim, J.-J. P. (1997). *Biochemistry*, **36**, 8455–8464.
Unno, H., Yamashita, S., Ikeda, Y., Sekiguchi, S.-Y., Yoshida, N., Yoshimura, T., Kusunoki, M., Nakayama, T., Nishino, T. & Hemmi, H. (2009). *J. Biol. Chem.* **284**, 9160–9167.
Urano, K., Daimon, T., Banno, Y., Mita, K., Terada, T., Shimizu, K., Katsuma, S. & Shimada, T. (2010). *FEBS J.* **277**, 4452–4463.
Weiss, M. S. (2001). *J. Appl. Cryst.* **34**, 130–135.
Winn, M. D. *et al.* (2011). *Acta Cryst.* D**67**, 235–242.
Wischgoll, S., Demmer, U., Warkentin, E., Günther, R., Boll, M. & Ermler, U. (2010). *Biochemistry*, **49**, 5350–5357.
Wischgoll, S., Taubert, M., Peters, F., Jehmlich, N., von Bergen, M. & Boll, M. (2009). *J. Bacteriol.* **191**, 4401–4409.
Wübbeler, J. H., Bruland, N., Kretschmer, K. & Steinbüchel, A. (2008). *Appl. Environ. Microbiol.* **74**, 4028–4035.
Wübbeler, J. H., Raberg, M., Brandt, U. & Steinbüchel, A. (2010). *Appl. Environ. Microbiol.* **76**, 7023–7028.
Ye, X., Ji, C., Zhou, C., Zeng, L., Gu, S., Ying, K., Xie, Y. & Mao, Y. (2004). *Mol. Biol. Rep.* **31**, 191–195.
Zschocke, J., Quak, E., Guldberg, P. & Hoffmann, G. F. (2000). *J. Med. Genet.* **37**, 177–181.